

## Fundus albipunctatus photoreceptor microstructure revealed using adaptive optics scanning light ophthalmoscopy

Ethan K. Sobol<sup>a,b,\*</sup>, Avnish Deobhakta<sup>a,b</sup>, Carl S. Wilkins<sup>a,b</sup>, Jasmine H. Francis<sup>c</sup>, Toco Y. P. Chui<sup>a</sup>, Alfredo Dubra<sup>d</sup>, Davis B. Zhou<sup>a</sup>, Maria V. Castanos<sup>a</sup>, Gareth M.C. Lema<sup>a,b</sup>, Richard B. Rosen<sup>a</sup>, Justin V. Migacz<sup>a</sup>

<sup>a</sup> Icahn School of Medicine at Mount Sinai and New York Eye and Ear Infirmary of Mount Sinai, Department of Ophthalmology, New York, NY, USA

<sup>b</sup> James J. Peters VA Medical Center, Department of Ophthalmology, Bronx, NY, USA

<sup>c</sup> Memorial Sloan Kettering Cancer Center, Ophthalmic Oncology Service, New York, NY, USA

<sup>d</sup> Department of Ophthalmology, Stanford University, Palo Alto, CA, USA

### ARTICLE INFO

#### Keywords:

Fundus albipunctatus  
Macular dystrophy  
Adaptive optics scanning laser ophthalmoscopy  
RDH5 retinopathy  
11-*cis* retinol dehydrogenase mutation  
High resolution *in vivo* imaging

### ABSTRACT

**Purpose:** Fundus albipunctatus is an inherited cause of congenital stationary night blindness. The objective of this report is to describe structural changes occurring in a macular phenotype of a novel RDH5 mutation producing fundus albipunctatus using high-resolution *in vivo* imaging. A 62-year-old male with longstanding night blindness underwent imaging and genetic evaluation. High-resolution images of the photoreceptor mosaic were compared to those of a healthy subject. Results of a comprehensive ophthalmic evaluation and genetic testing with imaging including fundus photography, spectral-domain optical coherence tomography (OCT), fluorescein angiography (FA), OCT angiography (OCT-A), and adaptive optics scanning light ophthalmoscopy (AOSLO) are described. **Observations:** The patient presented with visual acuity of 20/25 in both eyes and longstanding poor dark adaptation. Anterior segment examination was unremarkable. Fundoscopy revealed well circumscribed bilateral perifoveal mottling and atrophy in both eyes. Discrete white-yellow flecks were present beyond the vascular arcades extending to the far periphery. Genetic testing revealed a novel compound heterozygous RDH5 mutation (c.388C > T, p.Gln130\*; c.665T > C, p.Leu222Pro). OCT demonstrated perifoveal photoreceptor and outer retinal irregularities, which corresponded to a window defect with late staining on FA. OCT-A demonstrated normal retinal vasculature with patchy areas of non-perfusion in the choriocapillaris. Macular abnormalities in both eyes were imaged using AOSLO to assess cone and rod photoreceptor architecture. While clinical features are consistent with a primary rod disorder, confocal AOSLO showed a paucity of normal cones with a small spared central island in both eyes. Rods appeared larger and more irregular throughout the macula. Non-confocal split detection AOSLO imaging revealed the presence of cone inner segments in dark regions of confocal imaging, indicating some degree of photoreceptor preservation. **Conclusions and Importance:** The AOSLO imaging of this particular macular phenotype of fundus albipunctatus demonstrates some of the structural photoreceptor abnormalities that occur in this condition, adding insight to the variable presentation of RDH5 retinopathy. The presence of preserved inner segment architecture suggests the possibility that gene therapy could play a future role in treating this condition.

### 1. Introduction

Fundus albipunctatus is an autosomal recessive form of congenital stationary night blindness associated with 11-*cis* retinol dehydrogenase (RDH5) gene mutations. While phenotypic variability exists, the condition typically presents with numerous discrete white-yellow flecks in

the retinal periphery, which vary in shape and density among patients and according to age.<sup>1,2</sup> Classic descriptions include normal visual acuity, visual fields, and color vision, with a stationary component of impaired scotopic vision that improves following prolonged dark adaptation.<sup>3</sup> More recent reports describe variable macular dysfunction and cone dystrophy in older patients.<sup>4</sup> Physiologic studies have

\* Corresponding author. 1468 Madison Ave, Annenberg 22-86, New York, NY, 10029, USA.

E-mail address: [ethan.sobol@mountsinai.org](mailto:ethan.sobol@mountsinai.org) (E.K. Sobol).

<https://doi.org/10.1016/j.ajoc.2021.101090>

Received 13 October 2020; Accepted 12 April 2021

Available online 16 April 2021

2451-9936/© 2021 The Authors.

Published by Elsevier Inc.

This is an open access article under the CC BY-NC-ND license

(<http://creativecommons.org/licenses/by-nc-nd/4.0/>).

characterized these photopic abnormalities, while very few investigations have examined the structural details of photoreceptors in patients with significant maculopathy. This report describes the findings of *in-vivo* high-resolution imaging of the photoreceptor changes in fundus albipunctatus with macular dystrophy, which include a degree of structural preservation revealed by AOSLO.

### 1.1. Case report

A 62-year-old male presented with longstanding poor night vision, beginning around 8 years of age, and stable visual acuity with little symptomatic progression over many years. On the basis of the clinical appearance, the patient carried a diagnosis of Stargardt's disease without confirmatory genetic testing. He had no other past ocular or surgical history, denied any family history or use of any medications associated with ocular toxicity. His only past medical history included mild peripheral arterial disease. Review of systems was unremarkable for any systemic complaints.

Visual acuity was 20/25 in each eye. Pupillary examination and intraocular pressures were within normal limits. Ishihara color testing was reduced to six of 12 correct plates in each eye. The anterior segment was notable for mild nuclear sclerotic cataracts in both eyes. Fundoscopic examination revealed a clear vitreous with normal optic nerves and vasculature. In both eyes, there was a flat and well circumscribed area of perifoveal atrophy with retinal pigment epithelial (RPE) mottling (Fig. 1A). Discrete white-yellow flecks without areas of confluence were present peripheral to the vascular arcades, most dense in the mid peripheral retina (Fig. 1B). OCT revealed apparent elongation and splitting of the photoreceptors in areas of separation from the RPE, which itself had small variations in thickness and reflectance in the central macula, while the remaining inner retinal layers appeared normal (Fig. 1C). In the early phases of FA, hyperfluorescent areas appeared in the macula, which stained in later frames, corresponding to the atrophic bull's eye pattern visible on funduscopy (Fig. 1D). A granular staining was seen in the peripheral retina which appeared to coincide with retinal flecks. A 24–2 white stimulus III Humphrey visual field demonstrated bilateral central scotomas with intact foveal fixation. OCT-A confirmed normal retinal vasculature (Fig. 2A–C), with the exception of patchy areas of

non-perfusion at the level of the choriocapillaris (Fig. 2D). Genetic testing (Spark Therapeutics, Inherited Retinal Disease Panel, Philadelphia, PA, USA), revealed a novel compound heterozygous RDH5 mutation (c.388C > T, p.Gln130\*; c.665T > C, p.Leu222Pro), consistent with a diagnosis of autosomal recessive fundus albipunctatus.

Reflectance confocal AOSLO imaging of the photoreceptor mosaic showed central foveal preservation, with marked disruption in the surrounding area (Fig. 3A). Within the preserved foveal area, the cones appear larger and less densely packed when compared to a normal subject (Fig. 3B). The cones immediately outside of this area were also more sparse and darker in appearance. Non-confocal split-detection images were taken simultaneously and are co-registered with the confocal images (Fig. 3C and D). Split-detection images are believed to highlight translucent structures such as the inner segments of photoreceptors, and in this case the patient's image (Fig. 3C) indicates large intact inner segments in the areas immediately outside the spared foveal cones, and are of much larger and appear with higher contrast than the corresponding structures in a normal fovea (Fig. 3D). The *en face* perspective can also be shown with the OCT data (Fig. 4), where a 3  $\mu\text{m}$ -thick slab placed 40  $\mu\text{m}$  above the Bruch's membrane can clearly show the areas where photoreceptors are disrupted around the fovea. The region of spared foveal cones can be seen clearly in the center (Fig. 4B). In another confocal image at approximately two-thirds of the distance between the fovea and optic nerve (Fig. 5A), cones continue to appear larger than normal with an irregular distribution. The intervening rod cells, which are normally not well imaged in this area owing to their small size, were distinctly brighter than the surrounding disrupted cones and larger in diameter (Fig. 5A) when compared to those of normal eyes (Fig. 5B). Non-confocal split detection AOSLO images (Fig. 5C) revealed intact inner segments of some of the dark cone cells in the corresponding confocal images suggestive of partial preservation of photoreceptor architecture.

Details of the findings and the current absence of therapeutic options were discussed with the patient. He declined an offer of genetic counseling referral.

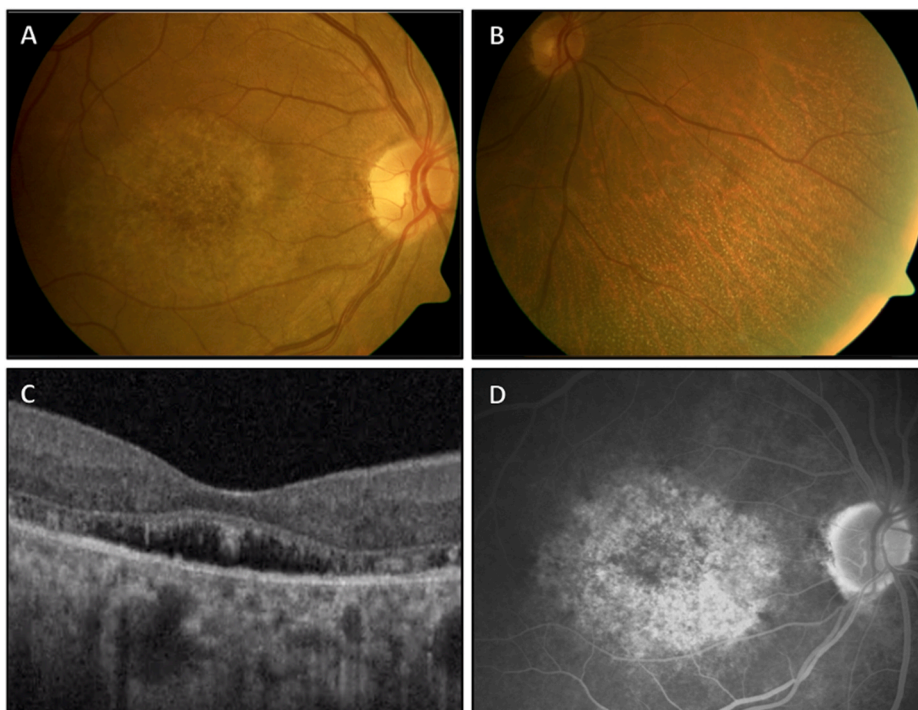


**Fig. 1.** Imaging of the right eye of a patient with fundus albipunctatus. A fundus photo (A) has an atrophic bull's eye pattern with retinal pigment epithelial (RPE) mottling confined to the perifoveal region. The nasal periphery (B) demonstrates discrete white-yellow flecks. Spectral domain OCT (C) (Optovue Avanti, 3 × 3mm) shows photoreceptor splitting and separation from the underlying RPE. The late phase FA (D) depicts stained fluorescence corresponding to the macular irregularities seen in (A). (For interpretation of the references to color in this figure legend, the reader is referred to the Web version of this article.)



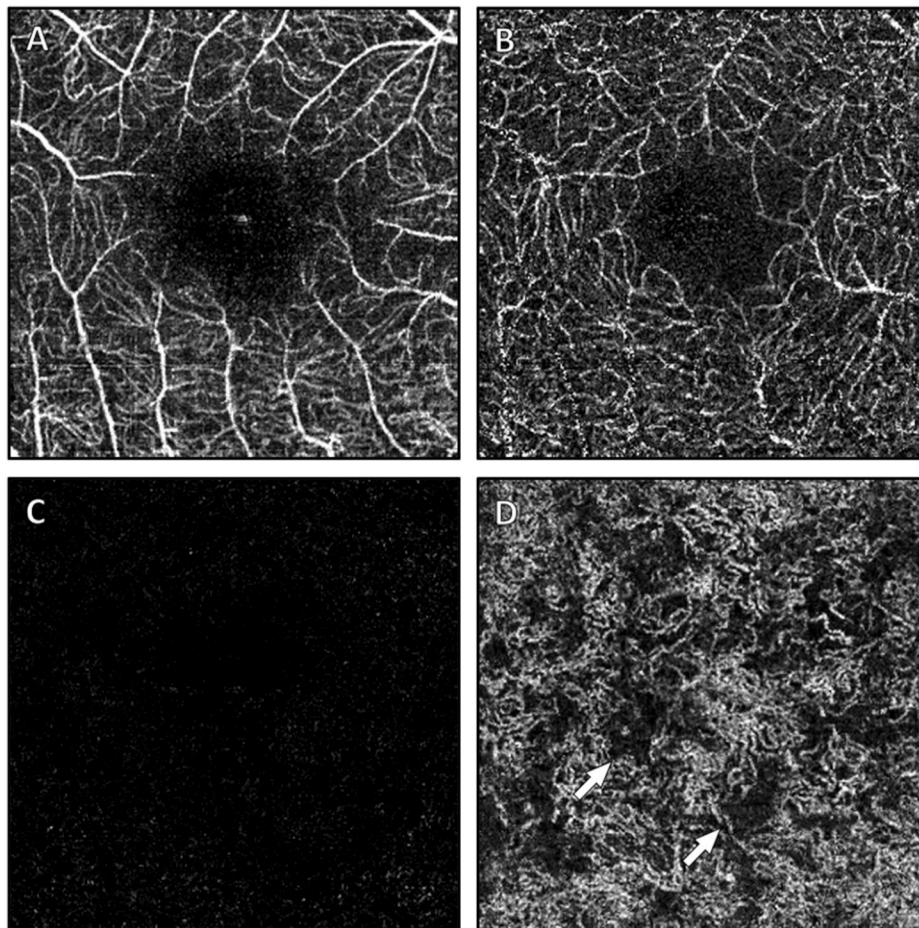


**Fig. 2.** Optical coherence tomography angiography at the macula (Optovue Avanti, 3 × 3mm). Vasculature in the superficial retina (A), deep inner retina (B), and outer retina (C) have a normal appearance, while at the level of the choriocapillaris (D) there are patchy areas of non-perfusion as indicated by the arrows.

## 2. Discussion

Fundus albipunctatus was initially described as a form of congenital stationary night blindness characterized by minimal progression over time.<sup>3</sup> However, cone dystrophy in a subset of patients has been reported, especially in older individuals.<sup>1</sup> It has been hypothesized that the progressive cone dysfunction seen in fundus albipunctatus may be related to impaired RPE function due to the RDH5 gene mutation, or from the direct effects of a depleted 11-*cis*-retinal supply to the cone cells.<sup>4</sup> Structural abnormalities have been described in the outer retina and photoreceptor inner segment-outer segment junction.<sup>2,5</sup> Ocular aberrations limit the ability to resolve the photoreceptors using conventional ophthalmic imaging devices. AOSLO provides greater detail in characterizing microstructural abnormalities of various retinal diseases.<sup>6,7,8,9</sup>

Previous studies of fundus albipunctatus patients with RDH5 mutations imaged with AOSLO have reported cone irregularities and mosaic disruptions even in patients with minimal or no visible macular pathology on funduscopy or OCT, with the conclusion that cones are both fewer in number and irregularly spaced.<sup>5,10</sup> These cone cell abnormalities may also represent early findings prior to progression to a macular phenotype, in contrast to the more advanced form seen in our patient in which the macular dystrophy was readily apparent on both clinical exam and multimodal imaging. While some variability has been described in the cone mosaic architecture and cell density even in normal subjects,<sup>11</sup> it is reasonable to conclude that the changes observed in the AOSLO confocal image of the cone mosaic of our patient are largely due to macular pathology.

Additionally, non-confocal split detection AOSLO imaging provides visualization of the mosaic of intact photoreceptor inner segments.<sup>12</sup> The split-detection images in our study suggest a partial preservation of photoreceptor inner segments despite their elongated and disrupted appearance on OCT, similar to previous reports.<sup>5,10</sup> In different retinal dystrophies, AOSLO reports have also described a similar structural preservation despite abnormal function<sup>13,14</sup>. This interpretation attributes the dark appearance of certain photoreceptors to a waveguiding dysfunction of metabolic origin without complete loss of the cell body.

Notably, while the patient's original diagnosis of Stargardt's disease was upended by genetic testing, the AOSLO findings are helpful for explaining the patient's clinical presentation. Previous studies using AOSLO in Stargardt's disease have revealed increased cone and rod spacing, with reduced foveal cone density and enlarged cone size, and dark cones thought to be associated with foreshortened outer segments<sup>15</sup>. These findings are similar to our patient's photoreceptor characteristics on AOSLO, except for the profound sparing observed in the central fovea. Indeed, AOSLO appears to be better able to characterize the photoreceptor status than traditional imaging modalities.<sup>7</sup>

Some limitations of our report include that it is based upon a single clinical subject and that we were unable to perform high-resolution AO imaging of the peripheral retinal flecks, which were located beyond the accessible field of the current AOSLO instrument. Electroretinographic studies may have provided further additional functional data but would offer little to the characterization of cone photoreceptor microstructure.

In summary, AOSLO imaging of this macular phenotype of fundus albipunctatus has demonstrated some of the structural photoreceptor abnormalities, which characterize RDH5 retinopathy. The finding of



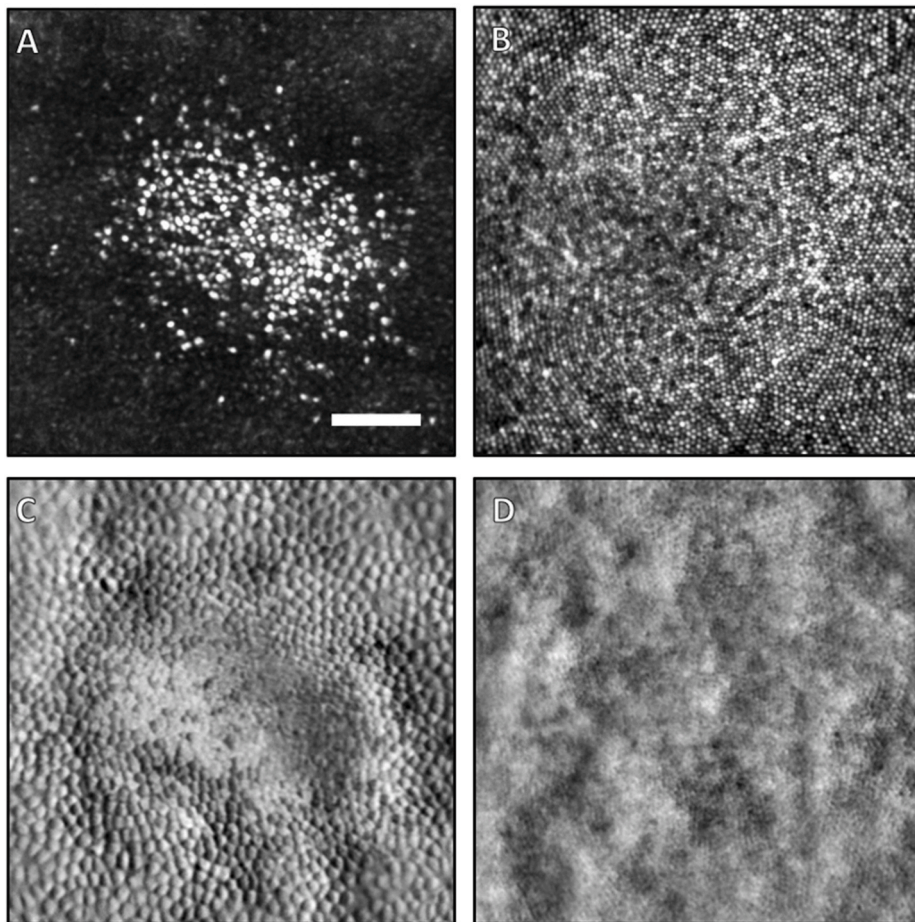


**Fig. 3.** AOSLO images ( $250\ \mu\text{m} \times 250\ \mu\text{m}$ ) of the cone photoreceptor mosaic in the central fovea of the right eye of the patient (A,C) and a healthy control (B,D). Both confocal scans (A,B) and non-confocal split detection images (C,D) are shown. In the patient, a small island of foveal cones are spared and have bright reflectivity compared to the surrounding cones (A). The patient's cones are also larger than the typical foveal cones of a normal subject (B). The most central cones of a typical healthy fovea are barely resolvable with this instrument. Simultaneously acquired non-confocal split-detection images, which normally depict the cone inner segment mosaic, of the patient (C) and healthy control (D) are shown. In the patient, the inner segments immediately outside the area of spared foveal cones appear larger and with much higher contrast than the fully intact cones (C). This difference in size and contrast is also apparent when comparing these inner segments to those of the healthy control (D). This increased contrast is an effect of the elevated height of these cones above the RPE, which amplifies the contrast in non-confocal split-detection imaging. The scale bar in (A) is  $50\ \mu\text{m}$ .

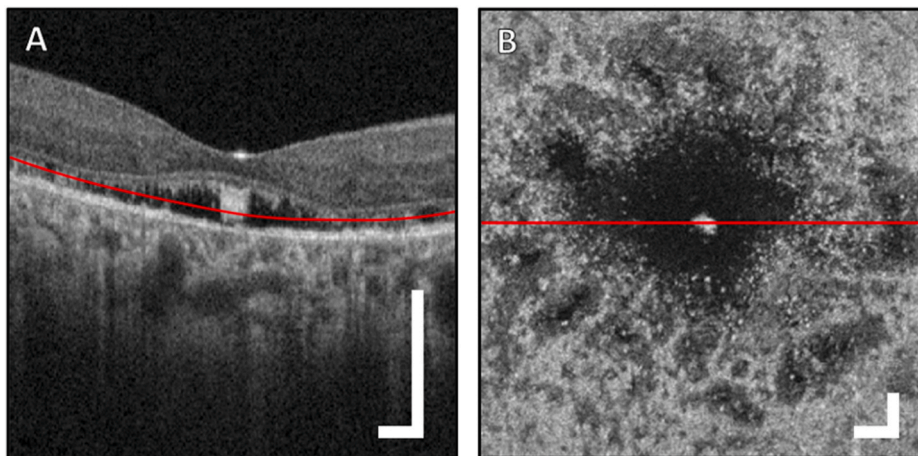


**Fig. 4.** Optical coherence tomography scan of the macula (Optovue Avanti; image dimensions,  $3 \times 3\text{mm}$ ). A B-scan through the fovea (A) and *en face* image (B) of the  $3\ \mu\text{m}$  thick projection extracted from the depth indicated by the red line in the B-scan (A). The red line in the *en face* projection (B) indicates the vertical location of the displayed B-scan from (A). In (B), a dark void surrounds the centrally spared foveal cones, thought to correspond with an area of reduced cone outer segment size. Peripheral to this area, there are patches of darkened reflectivity, likely representing variable cone integrity and a reduction in outer segment size. Scale bars are all  $300\ \mu\text{m}$ . (For interpretation of the references to color in this figure legend, the reader is referred to the Web version of this article.)

partial preservation of the photoreceptor inner segments despite an advanced macular dystrophy, indicates a persistence of structural integrity that could be amenable to future therapies.

#### Patient consent

Verbal consent of the patient and the healthy control were obtained for publication. This report does not contain any personal information that could lead to the identification of either the patient or the control.

#### Funding

This study was supported by the National Eye Institute of the National Institutes of Health under award numbers R01EY027301. The content is solely the responsibility of the authors and does not necessarily represent the official views of the National Institutes of Health. Additional funding for this research was provided by the New York Eye and Ear Infirmary Research Foundation and the Marrus Family Foundation. The sponsors and funding organizations had no role in the design or conduct of this research.

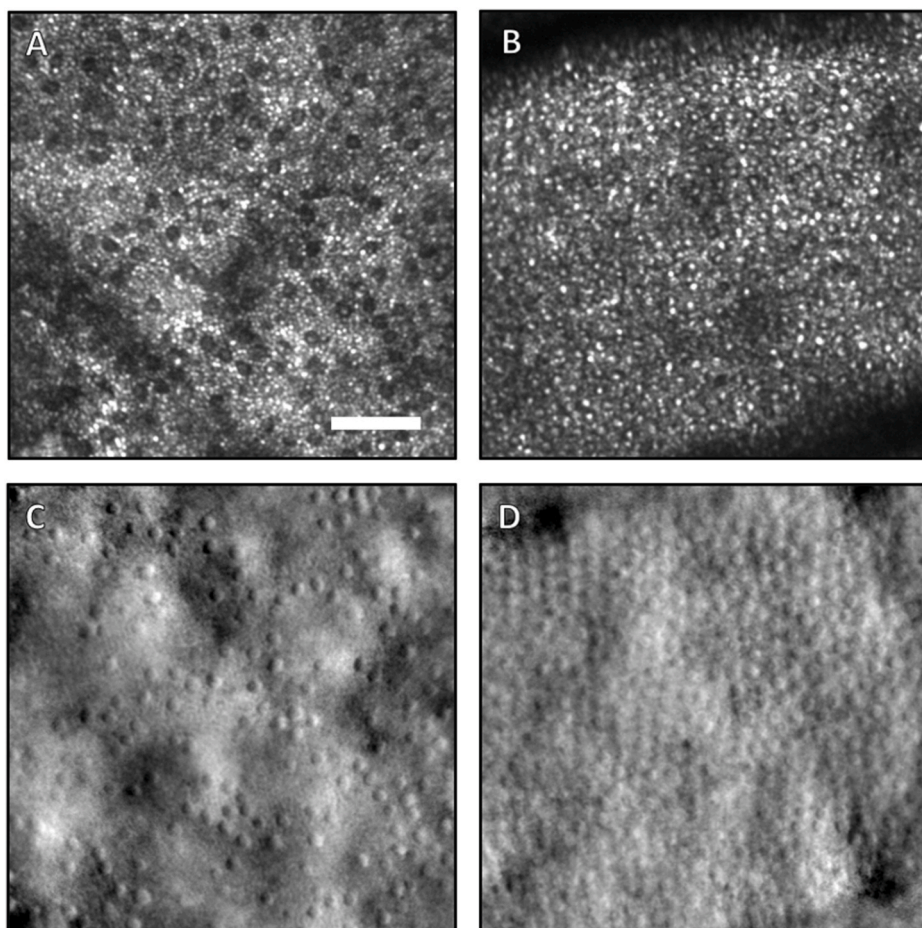


**Fig. 5.** AOSLO scans taken at retinal eccentricities of 10° nasal from the fovea in the right eye of both the patient (A,C) and the healthy control (B,D). The confocal scans are shown above (A,B) and the non-confocal split detection images are shown below (C, D). The patient has a degree of cone photoreceptor inner segment preservation in this nasal region which is just outside the macular lesion seen on fundus photography in Fig. 1. There is, however, a lower spatial density of these cells overall when compared to a similar location in the healthy control subject eye. Rod photoreceptors, which are smaller than cones, populate most of the area imaged. The rod size appears larger in (A) and their inner segments are more visible in (C) compared to a matched area in the healthy control subject's eye (D). In the normal control, the rod photoreceptor inner segments are not discernible from the large cones. Of note, the large dark lines in (A), (B), and (D) indicate shadow artifacts from large blood vessels and are normal features in AOSLO images. All scans are 250 μm by 250 μm, and the scale bar in (A) indicates a length of 50 μm.

### Conflicts of interest

Richard B. Rosen: OptoVue: Code C (Consultant); Boehringer-Ingelheim: Code C (Consultant); Astellas: Code C; Genentech-Roche: Code C; NanoRetina: Code C; OD-OS: Code C; Opticology: Code I (Personal Financial Interest); Guardion: Code I (Personal Financial Interest); Regeneron: Code C; Bayer: Code C.

The following authors have no financial disclosures: EKS, AD, CSW, JHF, TC, AD, DBZ, MVC, GL, JVM.

### Authorship

All authors attest that they meet the current ICMJE criteria for authorship.

### Acknowledgements

none.

### References

- Nakamura M, Hotta Y, Tanikawa A, Terasaki H, Miyake Y. A high association with cone dystrophy in fundus albipunctatus caused by mutations of the RDH5 gene. *Invest Ophthalmol Vis Sci.* 2000 Nov;41(12):3925–3932.
- Sergouniotis PI, Sohn EH, Li Z, McBain VA, et al. Phenotypic variability in RDH5 retinopathy (fundus albipunctatus). *Ophthalmology.* 2011 Aug;118(8):1661–1670.
- Marmor MF. Long-term follow-up of the physiologic abnormalities and fundus changes in fundus albipunctatus. *Ophthalmology.* 1990 Mar;97(3):380–384.
- Lidén M, Romert A, Tryggvason K, Persson B, Eriksson U. Biochemical defects in 11-cis-retinol dehydrogenase mutants associated with fundus albipunctatus. *J Biol Chem.* 2001 Dec 28;276(52):49251–49257.
- Makiyama Y, Ooto S, Hangai M, et al. Cone abnormalities in fundus albipunctatus associated with RDH5 mutations assessed using adaptive optics scanning laser ophthalmoscopy. *Am J Ophthalmol.* 2014 Mar;157(3):558–570.
- Burns SA, Elsner AE, Sapoznik KA. Adaptive optics imaging of the human retina. *Prog Retin Eye Res.* 2019 Jan;68:1–30.
- Georgiou M, Kalitzeos A, Patterson EJ. Adaptive optics imaging of inherited retinal diseases. *Br J Ophthalmol.* 2018;102:1028–1035.
- Liang J, Williams DR, Miller DT. Supernormal vision and high-resolution retinal imaging through adaptive optics. *JOSA A.* 1997;14(11):2884–2892.
- Roorda A, et al. Adaptive optics scanning laser ophthalmoscopy. *Opt Express.* 2002; 10(9):405–412.
- Song H, Latchney L, Williams D, Chung M. Fluorescence adaptive optics scanning laser ophthalmoscope for detection of reduced cones and hypoautofluorescent spots in fundus albipunctatus. *JAMA Ophthalmol.* 2014 Sep;132(9):1099–1104.
- Zhang T, Godara P, Blanco ER, et al. Variability in human cone topography assessed by adaptive optics scanning laser ophthalmoscopy. *Am J Ophthalmol.* 2015 Aug;160(2):290–300.
- Scoles D, Sulai Y, Langlo C, et al. In vivo imaging of human cone photoreceptor inner segments. *Invest Ophthalmol Vis Sci.* 2014;55(7):4244–4251.